Photo orientation of azo dye molecules in glassy *o*-terphenyl

S.Yu. Grebenkin *, B.V. Bol'shakov

Institute of Chemical Kinetics and Combustion, Institutskaya, 3, Novosibirsk 630090, Russian Federation

Abstract

A study was made of the formation of optical absorption anisotropy over the temperature range of 231.5–244 K in *o*-terphenyl, doped with an azo dye under linearly polarized light irradiation. The reorientation of dye molecules results from a succession of isomerization acts. The direction of a transition dipole upon isomerization for most of the molecules changes by angle of several degrees. A small fraction of molecules is characterized by a greater turn angle of approximately 37°.
© 2006 Elsevier B.V. All rights reserved.

Keywords: Optical anisotropy; Photo orientation; Azo dye; *o*-Terphenyl

1. Introduction

In the last decade, much attention has been focused on the photo orientation of dye molecules in solid matrices. The interest to this system is caused by its using for the creation of devices for the storage of information and other optical instruments. Many works devoted to this problem has been published. Most of the results obtained are included in the book of Sekkat and Knoll [1]. References in the present paper are not complete and reflect only the main aspects of the problem under study. The majority of studies are concerned with specially synthesized polymers in which a chromophor azo group is linked to the polymer chain [2–12], solutions of azo dyes in polymers [2,13–15] and layers containing azo dyes [16–18].

It is established that the photo orientation of dye molecules in polymers occurs during the reversible photoreaction of the *cis–trans* isomerization of azo molecules. The photo isomerization of *trans* molecules into the *cis* ones and vice versa occurs under irradiation with linearly polarized light in the absorption band of an azo compound. In this case, the dye molecules are oriented so that their transition dipoles tend to be in the plane which is perpendicular to the light polarization vector. The kinetics of photo orientation and the value of anisotropy depend substantially on a polymer structure [4,5,10–12,14] and relative rates of the photoinduced and dark isomerizations [6,10].

Much attention is paid to the study of the influence on the process of the photo orientation of polymer origin, the rigidity of its main chain, the origin of the link between azo chromophore and polymer chain, the value and distribution of a free polymer volume, and the temperature of polymer matrix vitrification. A theoretical description of the process of photo orientation kinetics by a system of integro-differential equations is presented [2,7,10,19]. The method of its solution is based on the expansion of the required functions in terms of Legendre polynomials. This allows one to compare in some cases theoretical curves with experimental results.

Although there is a great number of works, the mechanism of photo orientation is not clearly understood. In the present work, we have studied in detail the photoinduced formation of optical absorption anisotropy in the low-molecular weight matrix of *o*-terphenyl (OTP) doped with azo dye. It is shown that in this case, there is the process of the photo orientation of azo dye molecules. As in the case of polymers, photo orientation occurs upon the repeating cycles of *cis–trans* photo isomerization. A theoretical calculation of the evolution of optical anisotropy was performed to determine the kinematics of transition dipole rotation under light irradiation. We have derived explicit equations to describe the process in two cases: (i) the case of molecule rotation through a random angle, and (ii) the case of the turns of fixed values associated with each act of isomerization. The time dependence of the anisotropy was fitted by a numerical solution of a system of differential equations.

The photo orientation of azo molecules in low-molecular weight matrices was studied only in the 60-s by Stolbova and

---

* Corresponding author. Tel.: +7 3833333456; fax: 7 383 330 7350.
E-mail address: grebenk@ns.kinetics.nsc.ru (S.Yu. Grebenkin).

co-workers [20–22], who were the first to explain a given phenomenon. The study was carried out for the system azo dye–glycerol. The evolution of the photo orientation of azo dye molecules in low-molecular weight matrices has not been studied until now.

2. Experimental

2.1. Experimental setup

The anisotropy formation kinetics were monitored by measuring a sample absorbance (spectrophotometer SPECORD UV VIS, Carl Zeiss JENA) at a wavelength of absorption maximum of *trans* isomer (388 nm). Design of the spectrophotometer allows obtain absorbance values in a digital form. The sketch of the experimental setup is depicted in Fig. 1.

The temperature controlled (temperature controller Polikon 613, Thermex, S.-Petersburg) aluminium cell equipped with quartz windows for probe and photolytic beams was placed in the spectrophotometer. The cell was cooled by gaseous nitrogen evaporated in a Dewar flask and passed through the channels drilled in the cell walls. The sample temperature was kept constant to within ± 0.1 K. The measuring accuracy of temperature was ± 0.3 K.

A 500 W high-pressure mercury arc lamp (DRSh-500-2M) operating on direct current was used as a source of irradiation light. The time stability of light flux was $\pm 1\%$. The light intensity at 546 nm measured by the rate of azobenzene photo iso-merization in isooctane [23] was $(7.6 \pm 0.8) \times 10^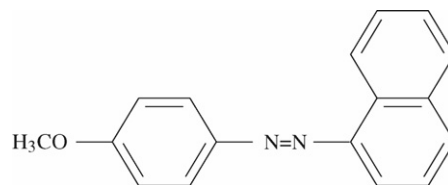{16}$ photons s^{-1} cm^{-2}. The required line of mercury spectrum was isolated by the standard set of glass filters immersed in water bath.

The light absorption by the sample at 546 nm does not exceed 1%. Therefore, the light intensity was considered constant throughout the sample.

To obtain a polarized light the polarizers from LOMO PLC were used. We experimentally determined that the contrast of the polarizers at 546 nm is more than 4.7×10^2. To polarize the probe beam the polarizer was installed directly behind the probe light source inside the spectrophotometer. A homemade holder allows two fixed positions of the polarizer at which probe light has either vertical or horizontal polarization. Because of light attenuation by polarizer, a more powerful incandescent lamp of 50 W (Royal Philips Electronics) was used as a probe light source. It takes about two seconds to change the orientation of the polarizer manually.

2.2. Sample preparation

The OTP powder (Fluka, $\geq 99.0\%$ (GC), mp 329–332 K) was used as recieved. Azo dye (1-naphthyl-azomethoxybenzene, NAMB) was synthesized in our lab in accordance with [24] and used after thin-layer chromatography purification. Its chemical structure is depicted in Fig. 2.

The OTP powder was placed in a Pyrex ampoule with a rectangular cross-section of 1 mm × 8 mm and a height of 15 mm. The OTP was melted in the ampoule and then the azo dye was dissolved there. The concentration of NAMB in solution was about 4×10^{-4} mol/l.

The ampoule with a solution was kept at 373–393 K during 1.5 h. After the warming no crystallization of OTP occurred at room temperature for several months.

After heating, the ampoule has been kept at room temperature for 3 min and then placed into the cell cooled to experimental temperature. The samples obtained in such a way did not crack and contained no bubbles. The ampoule was mounted in the cell so that the angles between the light beams and the plane of the face 15 × 8 were 45°. After 17 h of exposure at experimental temperature in darkness the anisotropy formation kinetics was measured. To create the anisotropy the sample was irradiated with vertically polarized light 546 nm.

The tetracene (UNION REAGENT) was used after recrystallization.

3. Results and discussion

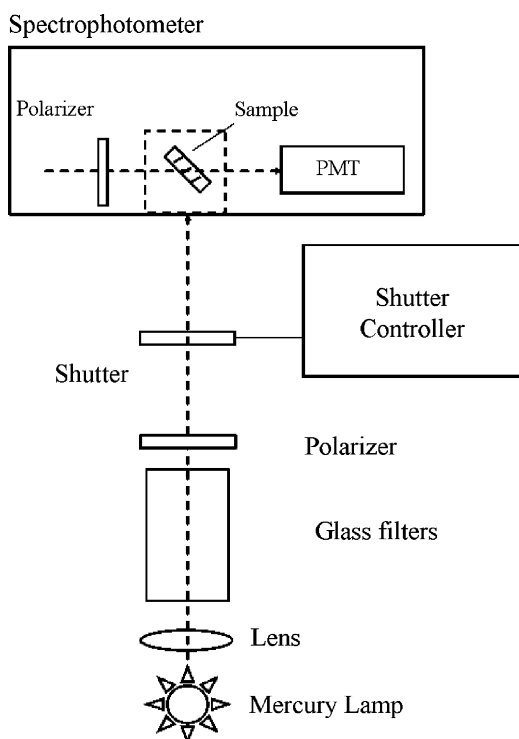Under light irradiation, the NAMB molecules undergo *cis–trans* isomerization. A photostationary content of isomers

Fig. 2. The chemical structure of NAMB.

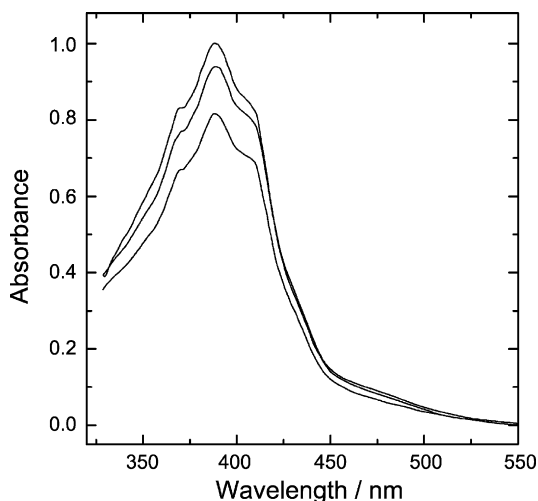Fig. 1. Schematic representation of the experimental setup.

Fig. 3. UV–vis absorption spectrums of NAMB in OTP before irradiation (top curve) and after 2.5 h of irradiation with vertically polarized light 546 nm (middle and bottom curves), 239 K. The polarization of the probe light is horizontal (middle curve) and vertical (bottom curve).

depends on the light wavelength. The dark $cis \rightarrow trans$ isomerization occurs with a noticeable rate near and above room temperature. In the temperature range, used in the present work, the rate of this process is negligibly low.

Fig. 3 shows the spectra of optical absorption of NAMB in OTP before and after irradiation of the sample with linearly polarized light (546 nm). A maximum of *trans* isomer absorption is at a wavelength of 388 nm. Light irradiation leads to a decrease in sample absorption over the *trans* isomer absorption range. As indicated by the figure, after irradiation with linearly polarized light, the sample absorption spectrum depends on the probing light polarization. The figure clearly demonstrates the appearance of optical absorption anisotropy upon *cis–trans* isomerization.

A quantitative description of experimental data was performed using the value of sample anisotropy which is defined as

$$A_0(t) = \frac{Abs_\perp(t) - Abs_\|(t)}{2Abs_\perp(0) + Abs_\|(0)}, \qquad (1)$$

where $Abs_\perp$ and $Abs_\|$ are the absorbances of the sample at 388 nm measured using the horizontal and vertical polarizations of probing light, respectively. As follows from Eq. (1), the $A_0(t)$ value is a one third of difference in the $Abs_\perp(t)$ and $Abs_\|(t)$ values normalized to the initial isotropic absorbance.

Formation of the optical absorption anisotropy has been studied over the temperature range of 231.5–244 K with a step of 2.5 K. The typical curves of anisotropy formation under sample irradiation with a vertically polarized light of 546 nm are shown in Fig. 4. The figure presents the experimental results that correspond to the extreme points of the temperature range studied. The curve of anisotropy formation at 231.5 nm was obtained in one measurement. The curve obtained at 244 K is the superposition of the data of two individual measurements.

Fig. 5a shows the time evolution of $Abs_\perp$ and $Abs_\|$ values at 239 K. A corresponding time dependence of anisotropy is

given in Fig. 5b. The $Abs_\|$ value decreases rapidly over the initial period of time. Under further irradiation, it continues to decrease but more slowly. The time dependence of $Abs_\perp$ value displays a minimum. A similar behavior of the $Abs_\perp$ and $Abs_\|$ values has been observed for polymeric systems [6,10].

Two possible explanations for the formation of optical anisotropy suppose the rotation of molecules as a whole in consequence of either (i) diffusion in *cis* and *trans* states, without rotation in photo isomerization process or (ii) rotation in photo
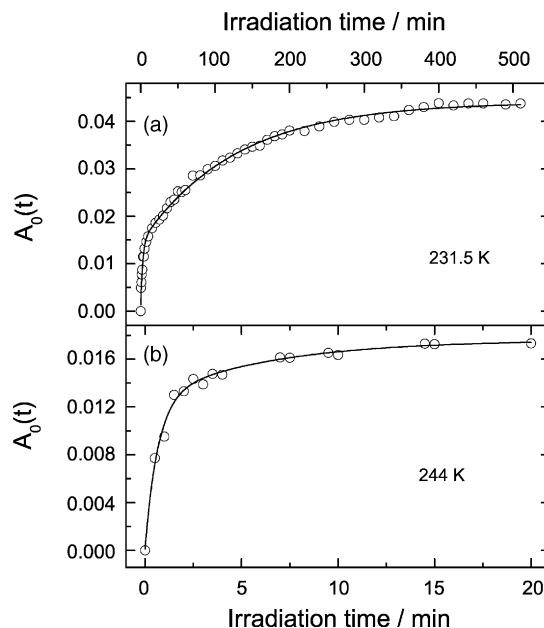

Fig. 4. Formation of the sample anisotropy under irradiation with the vertically polarized light 546 nm. The solid lines serve to guide the eyes.
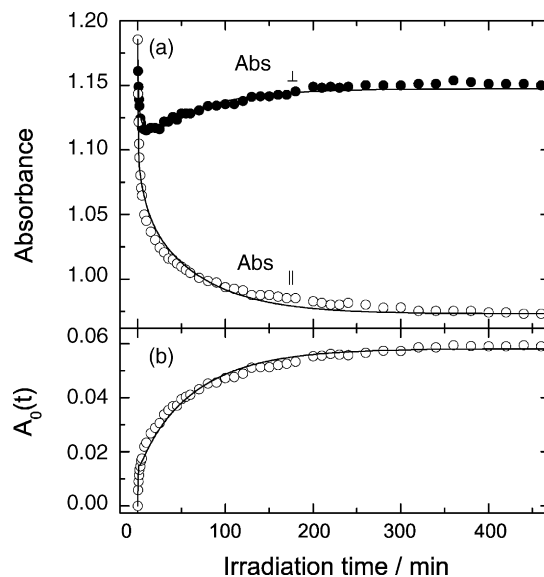

Fig. 5. (a) Absorption evolution of NAMB in OTP during irradiation with the vertically polarized light 546 nm, monitoring by horizontally (top curve) and vertically (bottom curve) polarized light. (b) Corresponding anisotropy formation curve, 239 K. Solid lines are fitting curves obtained using the *Model of fixed angle turns* and bimodal distribution of the dye molecules over the turn values (see text).

isomerization process, e.g., $trans(\theta_1) \rightarrow cis(\theta_2) \rightarrow trans(\theta_3) \rightarrow \cdots$, where θ_i is the angle between the direction of light polarization and the transition dipole of a dye molecule, $\theta_1 \neq \theta_3$.

Let us consider the first case. With the proviso that the coefficient of the rotational diffusion of *cis* particles exceeds a corresponding value for *trans* particles and *cis* particles are characterized by some isotropic proportion of absorption, a sequence of the processes:

(a) isomerization, $trans(\theta_1) \rightarrow cis(\theta_1)$,
(b) diffusion, $cis(\theta_1) \rightarrow cis(\theta_2)$,
(c) and back isomerization, $cis(\theta_2) \rightarrow trans(\theta_2)$,

can give rise to anisotropy. At the same time we suppose that *trans* particles absorb the light according to pure dipole transition mechanism. The calculation of absorbance evolution have been performed for this case using Eqs. (2).

$$
\begin{aligned}
\frac{dn_t(t,\theta)}{dt} &= -I\sigma_t\phi_{tc}\cos^2\theta\, n_t(t,\theta) + I\sigma_c\phi_{ct}(a+(1-a)\cos^2\theta)n_c(t,\theta) + D_{rot_t}\Delta n_t(t,\theta), \\
\frac{dn_c(t,\theta)}{dt} &= -I\sigma_c\phi_{ct}(a+(1-a)\cos^2\theta)n_c(t,\theta) + I\sigma_t\phi_{tc}\cos^2\theta\, n_t(t,\theta) + D_{rot_c}\Delta n_c(t,\theta).
\end{aligned}
\tag{2}
$$

The initial conditions are

$$
n_t(0,\theta) = \frac{1}{4\pi}, \qquad n_c(0,\theta) = 0. \tag{3}
$$

Here and below, we follow the next notations: θ is the angle between the direction of light polarization (Z-axis) and the transition dipole of a dye molecule, $n_t(t,\theta)$, $n_c(t,\theta)$ the angle distribution functions for *trans* and *cis* molecules; due to axial symmetry these functions do not depend on the axial angle φ, I is the light intensity, σ_t, σ_c the absorption cross-sections of *trans* and *cis* isomers at wavelength of photolysis, when $\theta = 0$, ϕ_{tc}, ϕ_{ct} are the quantum yields of $trans \rightarrow cis$ and $cis \rightarrow trans$ isomerization, respectively, a is the proportion of isotropic absorption of *cis* isomer, D_{rot_t}, D_{rot_c} the rotational diffusion coefficients of *trans* and *cis* isomers and Δ is the Laplacian.

The balance equation hold for the angle distribution functions:

$$
\int_0^{2\pi}\int_0^{\pi}(n_t(t,\theta)+n_c(t,\theta))\sin\theta\,d\theta\,d\varphi = 1. \tag{4}
$$

A more than three-fold difference in rotational diffusion coefficients of *cis* and *trans* molecules raises doubts. Actually, the three-fold difference in the rotational times was observed for the molecules which strongly differ in their size, e.g., anthracene and anthanthrene [25]. The sizes of NAMB isomers differ to a lesser extent, therefore hardly theirs rotational diffusion coefficients differ so strongly. Moreover, the molar volume, for example, of *cis* stilbene, a molecule which structure is close to structure of azobenzene, in solution is larger than that of *trans* stilbene [26].

Therefore, we conclude that the optical anisotropy of the sample is formed rather by the series of photo transformations. At the same time, we assume that the above-stated mechanism in some extent can also yield anisotropy of OTP matrix doped with NAMB.

The question about the angle value through which the NAMB molecule rotates upon photo isomerization calls for special studying. Let us consider two models corresponding to the simplest cases. In the framework of the first model, the direction of transition dipole changes randomly with isomerization and a new direction is equiprobable. The second model assumes a change in the transition dipole direction by a fixed angle value.

3.1. Model of random turns (RT)

We assume that rotation is performed with equal probability through any angle, i.e., orientation of the product is quite random. Since glass is an isotropic medium, in the process under study, all directions of spatial reorientation are equivalent. Let axis Z be directed along the vector of irradiating light polarization. Taking into account the process of thermal rotational diffusion, the evolution of the orientational distribution function for the molecules in the *trans* and *cis* states will obey the set of Eq. (5). Similar equations in the general case were used earlier in the works [2,7,10].

$$
\begin{aligned}
\frac{dn_t(t,\theta)}{dt} &= -I\sigma_t\phi_{tc}\cos^2\theta\, n_t(t,\theta) + I\sigma_c\phi_{ct}\int_0^{\pi/2}\cos^2\theta'\, n_c(t,\theta')\sin\theta'\,d\theta' + D_{rot}\Delta n_t(t,\theta), \\
\frac{dn_c(t,\theta)}{dt} &= -I\sigma_c\phi_{ct}\cos^2\theta\, n_c(t,\theta) + I\sigma_t\phi_{tc}\int_0^{\pi/2}\cos^2\theta'\, n_t(t,\theta')\sin\theta'\,d\theta' + D_{rot}\Delta n_c(t,\theta).
\end{aligned}
\tag{5}
$$

The first and second terms in the right-hand sides of Eq. (2) correspond to the disappearance and production of the molecules in a given conformation due to photo isomerization. The third term describes the rotational diffusion of molecules.

The fitting parameters which provide the best fitting result are: $D_{rot_c} = 1.1 \times 10^{-4}\,s^{-1}$, $D_{rot_t} = 3.2 \times 10^{-5}\,s^{-1}$, and $a = 0.15$. At that, the calculated results agree well with the experimental absorbance curves.

The initial conditions are set by Eq. (3). D_{rot} is the rotational diffusion coefficient of dye molecules. It is assumed that the coefficients of the rotational diffusion of *trans* and *cis* molecules are the same. The use of the identical coefficients of rotational diffusion for *trans* and *cis* isomers is an approximation. We assume that the molar volumes of *cis* and *trans* isomers of NAMB and hence its diffusion constants do not differ essentially. The validity of this assumption is supported by the reasons discussed above.
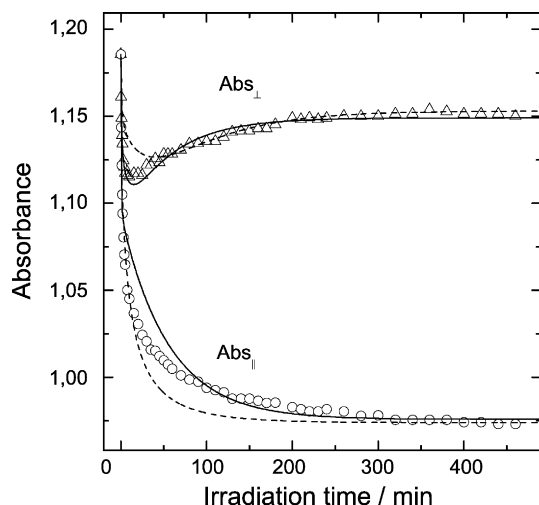
Fig. 6. Demonstration of fitting quality using different models. The dash and solid curves represent the fitting with the *Model of random turns*, and *Model of fixed angle turns*, respectively, 239 K.

The numerical calculations indicate that system of Eq. (5) fails to give even a rough description of experimental results. Thus, the assumption of the equiprobable turns of the NAMB molecules upon photo isomerization does not represent the facts.

To get a better description of experimental data by the *Model of random turns* we have introduced limitations to the area of the available transition dipole directions of the dye molecule in Eq. (5). We divided the total range of polar angle θ into N equal parts and assume that the transition dipole with the polar angle θ of the range between $\pi n/N$ and $\pi(n+1)/N$ can fall, after photo isomerization, at any point of the same range.

The best fitting of the theoretical curve in the framework of this model is achieved at $N = 6$. The corresponding curve is shown in Fig. 6 by the dash line. As follows from the figure, the model mainly reflects all peculiarities of the time dependencies of $Abs_\perp$ and $Abs_{||}$. In this case, however, it predicts a faster reorientation of NAMB molecules. Indeed, the calculated $Abs_{||}$ values are strictly lower than the experimental points in the time range of 25–200 min. For the same reason, the calculated values of $Abs_\perp$ corresponding to the beginning of the process, exceed the experimental values. The results obtained indicate that the contribution of turns by large angles in this model is too great.

3.2. Model of fixed angle turns (FT)

In this model, transition dipoles turns is performed through fixed angle α. This idea was used also by Sekkat et al. in the work [7]. The orientational distribution function for the *trans* isomer obeys to equation (see Appendix A)

$$\frac{dn_t(t, \theta)}{dt} = -I\sigma_t\phi_{tc}\cos^2\theta\, n_t(t, \theta) + \frac{I\sigma_c\phi_{ct}}{\pi}\int_{|\theta-\alpha|}^{\theta+\alpha} n_c(t, \theta')$$

$$\times \frac{\cos^2\theta'\,\sin\theta'\,d\theta'}{\sqrt{\sin^2\alpha\,\sin^2\theta' - (\cos\theta - \cos\alpha\,\cos\theta')^2}}$$

$$+ D_{rot}\Delta n_t(t, \theta). \tag{6}$$

The same equation can be given for the distribution function of *cis* isomer. The initial conditions are set by Eq. (3).

Eq. (6) together with similar equation for $n_c(t,\theta)$ allow numerical computations of the distribution functions, $n_t(t,\theta)$ and $n_c(t,\theta)$ at any moment of time. To fit the experimental curves, the values $k_t \equiv I \times \sigma_t \times \phi_{tc}$, $k_c \equiv I \times \sigma_c \times \phi_{ct}$, α and D_{rot} were used as fitting parameters. The best fitting result obtained at $\alpha = 3.6°$ is shown in Fig. 6 by solid lines. As follows from the figure, the model *FT* give a better agreement with experimental results than the model *RT*. However, the noticeable deviations of the calculated values of $Abs_{||}$ from the experimental points are observed at times shorter than 80 min. This disagreement is caused by too slow reorientation of molecules in the framework of a given model. The attempt to increase the reorientation rate by increasing the value of the turn worsens the quality of the fitting.

The description of experimental curves was essentially improved by using a bimodal distribution of NAMB molecules over the values of rotation angle. The dynamics of molecules in each ensemble was described by the model *FT*. The ensembles were assumed not to mix together. A small fraction of NAMB molecules with a large rotation angle α_2 was added to the main ensemble of NAMB molecules with small rotation angle α_1. All fitting parameters were the same for both ensembles but value of rotation angle. Fig. 5 demonstrates good description of experimental data at 239 K when $\alpha_1 = 3.6°$ and $\alpha_2 = 29.1°$.

It is worth noting that a real distribution function over the values of rotation angle is, probably, a smooth angle function. Substituting this function by bimodal distribution is the approximation. A fairly good description of experimental curves in the framework of this approximation is likely to indicate that a real distribution function has a fairly sharp maximum near the determined value of the angle α_1 and a wing which gradually tends to zero toward large angles. The change in the α_2 value from 29.1° to 45° leads to a negligible change in the weight of the second ensemble and has a small effect on the kinetic curves. Therefore, we estimate the value α_2 to be $37 \pm 10°$.

Table 1 summarizes the values of fitting parameters obtained using the *FT* model and a bimodal distribution of the molecules over the values of turn angle for several temperatures. The k_c value of 7.5×10^{-2} s^{-1} was obtained by the fitting of the kinetic curves of the anisotropy formation at 239 K. This value was used as a fixed parameter when fitting at other temperatures. This approach is based on absence of temperature dependence of the rate of *cis* → *trans* photo isomerization whereas the rate of reverse process is strongly dependent on temperature [27]. As follows from the Table 1, the weight of the second ensemble is very small. This indicates that in most of the cases, the transition dipole turns in consequence of isomerization through about the same angle. The determined rotational diffusion coefficients D_{rot} agree very closely with that determined from anisotropy decay measurements for NAMB in OTP [28]. The values D_{rot}^* determined in these measurements are listed in the table.

3.3. Does light energy enhance the rotation?

It may be suggested that a dissipation of energy of the photon absorbed by a dye molecule causes a local "melting" of the

Table 1
Fitting parameters obtained using the *Model of fixed angle turns*

T (K)	k_t (10^{-3} s^{-1})[a]	D_{rot} (10^{-5} s^{-1})	D_{rot}^* (10^{-5} s^{-1})[b]	α_1 (°)	α_2 (°)	W_1[c]
236.5	6.7	1.4	1.4	2.7	29.1 (fixed)	0.95
239	8.2	3.5	4.5	3.6	29.1	0.947
241.5	12.6	19.0	29.0	6.3	29.1 (fixed)	0.985

[a] $k_t \equiv I \times \sigma_t \times \phi_{tc}$.
[b] D_{rot}^* is a value of rotational diffusion coefficient determined from anisotropy decay measurements.
[c] W_1 is weight of the first ensemble.

matrix. As a result, the rotational mobility of the dye molecule increases. The existence of such a mechanism was verified experimentally using tetracene. The size of the molecule of tetracene is close to that of the NAMB molecule but it undergoes no conformational transformations. Since the light with a wavelength of 546 nm is weakly absorbed by tetracene the sample was irradiated with light of a wavelength of either 405 or 436 nm. The sample absorbance was measured at a wavelength of one of the tetracene absorption maxima (397 nm).

The irradiation of the tetracene-containing sample at 436 nm for 160 min fails to give rise to optical absorption anisotropy. There are two reasons for that: (i) light does not stimulate a rotation, (ii) quantity of light energy transformed by tetracene molecule into heat per a second, Q_{tetr}, is too small. Let us compare the value Q_{tetr} with the energy dissipated into a matrix by the NAMB molecule. The value Q_{tetr} is given by

$$Q_{tetr} = I\sigma_{tetr}(1 - \phi_F), \tag{7}$$

where ϕ_F is the quantum yield of the fluorescence of tetracene.

The used light fluxes at 436 and 546 nm are comparable in their values.

The absorption cross-section of NAMB at 546 nm was estimated to be less than that of tetracene at 436 nm by a factor of approximately 10. The absorption cross-section of tetracene was estimated using the qualitative absorption spectrum measured by us and the literature value of this value at 472 nm [29].

The quantum yield of tetracene fluorescence in ethanol and benzene at room temperature is about 0.16 [30]. We have failed to find in the literature the data on tetracene fluorescence at 236.5 K or at close temperatures. The data of [31] testify to a negligible change in the value of the quantum yield of anthracene fluorescence in 2-methylpentane and ethanol in the temperature range of 235–300 K ($\phi_F \approx 0.3$). We assume that there are no strong variations in the quantum yield of tetracene fluorescence due to a decrease in temperature (from room temperature to 236.5 K). Thus, the main of the photon energy after light absorption by tetracene dissipates into heat.

It is concluded then that the amount of light energy converted by the tetracene molecule per second into heat upon light absorption at 436 nm is not smaller than the amount of heat released by the NAMB molecule upon light absorption at 546 nm.

The irradiation at 405 nm for 65 min gives anisotropy of 5×10^{-3} which is much smaller than the anisotropy observed for NAMB. The optical density for both the vertical and horizontal polarized light decreases monotonically with the formation of absorption anisotropy. This indicates that the appearance of

anisotropy is determined, in this case, by a selective photodecomposition rather than the rotation of tetracene molecules. This conclusion about the mechanism of the appearance of anisotropic distribution of tetracene molecules in OTP under linearly polarized light irradiation is confirmed by the work [32].

Thus, the release of the absorbed light energy into OTP matrix is likely to cause no rotation of absorbing molecules.

4. Conclusions

Irradiating azo dye solution in glassy OTP with linearly polarized light gives rise to the optical absorption anisotropy of a sample. This is induced by the rotation of dye molecules in consequence of the reverse *cis* ↔ *trans* photo isomerization. The photostimulated turns of the transition dipoles of most of the molecules in OTP matrix is likely to occur with approximately equal steps of several degrees in each act of photo isomerization. The transition dipoles of a small fraction of molecules turn through angle of $37 \pm 10°$. The dissipation of the absorbed photon energy does not, probably, stimulate the rotation of molecules in glassy OTP.

Acknowledgements

Appendix A. Model of fixed angle turns: the deduction of an equation for the orientational distribution function

Assume that axis Z is directed along the light polarization vector. Because of axial symmetry, the angular distribution of particle orientations depends only on the polar angle θ. The angle between the vectors of transition dipoles of the product and the precursor molecules upon isomerization is denoted by α. For simplicity, we assume that the vector of the transition dipole turns through the same angle both in consequence of *trans* → *cis* and *cis* → *trans* processes.

The number of *trans* molecules, whose direction of the transition dipole is characterized by the angle θ decreases due to the *trans* → *cis* isomerization and increases due to the reverse process. Only the *cis* molecules which has the transition dipole orientation in the range from $|\theta - \alpha|$ to $\theta + \alpha$ yield the increase of this number. For *trans* molecules, the time dependence of the
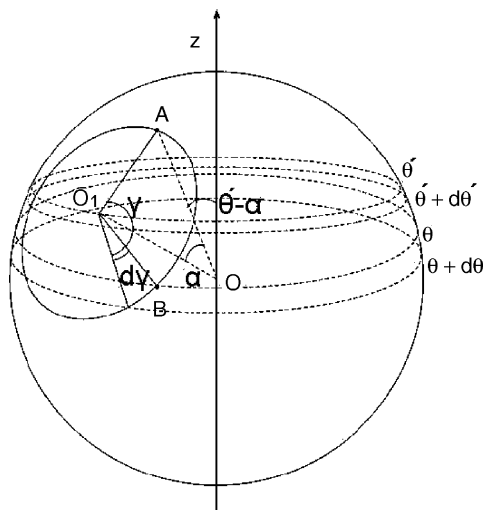
Fig. A1. Illustration for derivation of Eq. (6).

orientational distribution function $n_t(t, \theta)$ follows the equation

$$\frac{d}{dt} \int_{\varphi=0}^{2\pi} n_t(t, \theta) \sin \theta \, d\theta \, d\varphi$$

$$= -I\sigma_t\phi_{tc} \cos^2 \theta \int_{\varphi=0}^{2\pi} n_t(t, \theta) \sin \theta \, d\theta \, d\varphi + I\sigma_c\phi_{ct}$$

$$\times \int_{\varphi=0}^{2\pi} \int_{\theta'=|\theta-\alpha|}^{\theta'=\theta+\alpha} n_c(t, \theta') \cos^2 \theta' \sin^2 \theta' \, dw(\theta', \theta) \, d\theta' \, d\varphi.$$

$$(A.1)$$

In the left-hand side of the equation, there is the rate of a change in the probability to find the transition dipole of *trans* molecule in the range from θ to $\theta + d\theta$. In the right-hand side, the first term describes a decrease of this probability due to *trans* → *cis* photo isomerization and the second term describes an increase of that due to *cis* → *trans* isomerization. The factor $dw(\theta', \theta)$ is the probability that a *cis* particle characterized by a orientation within the angle range $\theta' - \theta' + d\theta'$ will transform into the *trans* particle having transition dipole direction in a range from θ to $\theta + d\theta$. The factor $dw(\theta', \theta)$ is of the form

$$dw(\theta', \theta) = \frac{d\gamma(\theta', \theta)}{\pi}. \qquad (A.2)$$

where $d\gamma(\theta', \theta)$ is the angle denoted in Fig. A1. In this figure, the circle with center point O_1 lies on the sphere of a unit radius and denotes all possible directions of *trans* dipole resulting from isomerization of the *cis* molecules whose dipoles directions are passing through the point O_1.

The angle between the ray OO_1 and a ray passing through O and any point of this circle is α. The angle γ corresponds to the arc of the circle between its upper point A and the point characterized by angle θ (point B). The angles θ, θ', α and γ are related by the equation

$$\cos \theta = \cos \alpha \cos \theta' + \sin \alpha \sin \theta' \cos \gamma. \qquad (A.3)$$

Differentiating Eq. (A.3) at constant α and θ', we get:

$$d\gamma(\theta', \theta) = \frac{\sin \theta \, d\theta}{\sin \alpha \, \sin \theta' \, \sin \gamma}. \qquad (A.4)$$

Expressing $\sin \gamma$ in terms of Eq. (A.3) and substituting it to Eq. (A.4), we obtain:

$$d\gamma(\theta', \theta) = \frac{\sin \theta \, d\theta}{\sqrt{\sin^2\alpha \, \sin^2 \theta' - (\cos \theta - \cos \alpha \, \cos \theta')^2}}. \qquad (A.5)$$

Integrating Eq. (A.1) over φ, using Eqs. (A.2) and (A.5) and adding the term responsible for rotational diffusion, we obtain:

$$\frac{dn_t(t, \theta)}{dt} = -I\phi_{tc}\sigma_t \cos^2 \theta \, n_t(t, \theta) + \frac{I\phi_{ct}\sigma_c}{\pi} \int_{|\theta-\alpha|}^{\theta+\alpha} n_c(t, \theta')$$

$$\times \frac{\cos^2 \theta' \, \sin \theta' \, d\theta'}{\sqrt{\sin^2 \alpha \, \sin^2 \theta' - (\cos \theta - \cos \alpha \, \cos \theta')^2}}$$

$$+ D_{rot}\Delta n_t(t, \theta). \qquad (A.6)$$

References

[1] Z. Sekkat, W. Knoll (Eds.), Photoreactive Organic Thin Films, Academic Press, San Diego, CA, 2002.
[2] M. Dumont, A. El Osman, Chem. Phys. 245 (1999) 437.
[3] A. Stracke, A. Bayer, S. Zimmermann, J.H. Wendorff, W. Wirges, S. Bauer-Gogonea, S. Bauer, R. Gerhard-Multhaupt, J. Phys. D: Appl. Phys. 32 (1999) 2996.
[4] D. Brown, A. Natansohn, P. Rochon, Macromolecules 28 (1995) 6116.
[5] X. Meng, A. Natansohn, P. Rochon, Polymer 38 (1997) 2677.
[6] K. Tawa, N. Zettsu, K. Minematsu, K. Ohta, A. Namba, Q. Tran-Cong, J. Photochem. Photobiol. A 143 (2001) 31.
[7] Z. Sekkat, J. Wood, W. Knoll, J. Phys. Chem. 99 (1995) 17226.
[8] Z. Sekkat, J. Wood, W. Knoll, W. Volksen, R.D. Miller, A. Knoesen, J. Opt. Soc. Am. B 14 (1997) 829.
[9] Z. Sekkat, Ph. Pretre, A. Knoesen, W. Volksen, V.Y. Lee, R.D. Miller, J. Wood, W. Knoll, J. Opt. Soc. Am. B 15 (1998) 401.
[10] Z. Sekkat, D. Yasumatsu, S. Kawata, J. Phys. Chem. B 106 (2002) 12407.
[11] J. Stumpe, L. Lasker, Th. Fischer, M. Rutloh, S. Kostromin, R. Ruhmann, Thin Solid Films 284–285 (1996) 252.
[12] C. Kempe, M. Rutloh, J. Stumpe, J. Phys.: Condens. Matter 15 (2003) S813.
[13] P. Wu, R. Philip, R.B. Laghumavarapu, J. Devulapalli, D.V.G.L.N. Rao, B.R. Kimball, M. Nakashima, B.S. DeCristofano, Appl. Opt. 42 (2003) 4560.
[14] K. Tawa, K. Kamada, T. Sakaguchi, K. Ohta, Polymer 41 (2000) 3235.
[15] K. Tawa, K. Kamada, K. Ohta, J. Photochem. Photobiol. A 134 (2000) 185.
[16] Z. Sekkat, J. Wood, Y. Geerts, A. El Meskini, M. Buchel, W. Knoll, Synth. Met. 81 (1996) 281.
[17] E. Wolarz, Th. Fischer, J. Stumpe, Thin Solid Films 424 (2003) 179.
[18] B.-D. Jung, J. Stumpe, J.D. Hong, Thin Solid Films 441 (2003) 261.
[19] H. Ishitobi, Z. Sekkat, S. Kawata, Chem. Phys. Lett. 316 (2000) 578.
[20] B. Neporent, O. Stolbova, Opt. Spectrosc. 10 (1961) 287.
[21] A. Makushenko, B. Neporent, O. Stolbova, Opt. Spectrosc. 31 (1971) 557.
[22] A. Makushenko, B. Neporent, O. Stolbova, Opt. Spectrosc. 31 (1971) 741.
[23] G. Zimmerman, L. Chow, U. Paik, J. Am. Chem. Soc. 80 (1958) 3528.
[24] H. Becker, W. Berger, G. Domschke, E. Fanghanel, J. Faust, M. Fischer, F. Gentz, K. Gewald, R. Gluch, R. Mayer, K. Muller, D. Pavel, H. Schmidt, K. Schollberg, K. Schwetlick, E. Seiler, G. Zeppenfeld, Organicum, 15th ed., VEB Deutscher Verlag der Wissenschaften, Berlin, 1976.

[25] M.T. Cicerone, F.R. Blackburn, M.D. Ediger, J. Chem. Phys. 102 (1995) 471.

[26] D. Gegiou, K.A. Muszkat, E. Fischer, J. Am. Chem. Soc. 90 (1968) 12.

[27] E. Fischer, J. Am. Chem. Soc. 82 (1960) 3249.

[28] S.Y. Grebenkin, B.V. Bol'shakov, J. Phys. Chem. B 110 (2006) 8582.

[29] J.B. Birks, Photophysics of Aromatic Molecules, Wiley/Interscience, J. Wiley & Sons Ltd., 1970.

[30] A. Kearval, F. Wilkinson, Chem. Phys. Lett. 11 (1971) 472.

[31] G. Greiner, J. Photochem. Photobiol. A 137 (2000) 1.

[32] M.T. Cicerone, M.D. Ediger, J. Phys. Chem. 97 (1993) 10489.